

Semileptonic $D_{(s)} \rightarrow A\ell^+\nu$ and nonleptonic $D \rightarrow K_1(1270, 1400)\pi$ decays in LCSR

S. Momeni*, R. Khosravi†

Department of Physics, Isfahan University of Technology, Isfahan 84156-83111, Iran

In this work, the transition form factors are calculated for the semileptonic $D_{(s)} \rightarrow A\ell^+\nu$ where $A = a_1, b_1, K_1(1270, 1400)$, i.e., $D^+ \rightarrow a_1^0(b_1^0, K_1^0)\ell^+\nu$, $D^0 \rightarrow a_1^-(b_1^-)\ell^+\nu$, and $D_s^+ \rightarrow K_1^0\ell^+\nu$ in the frame work of the light-cone QCD sum rules (LCSR) approach up to the twist-3 distribution amplitudes (DAs). Since the masses of these axial vector mesons are comparable to the charm quark mass, we keep out in our calculations all terms including m_A/m_c in expansion of two-parton DAs. Branching ratio values are estimated for the semileptonic $D_{(s)} \rightarrow A\ell\nu$ and nonleptonic $D \rightarrow K_1(1270, 1400)\pi$ decays. A comparison is also made between our results and predictions of other methods and the existing experimental values.

I. INTRODUCTION

Exclusive semileptonic decays of B and D mesons are very useful to determine the weak interaction couplings of quarks within the standard model (SM) because of their relative abundance and the simplicity of their study comparative to nonleptonic decays. In connection with the charmed hadrons, there are several features that make a difference between them and other hadrons. In the following, some of them are mentioned [1]:

- 1) The mass of the charmed hadrons is about 2 GeV. In these region, the nonperturbative hadronic physics is operative. However, theoretical methods developed for heavy quarks can in principle still be applied, albeit with larger uncertainties.
- 2) Charmed hadron data can be used to probe the Yukawa sector of the SM by the lattice QCD simulations.
- 3) In many cases, charm transitions provide almost background-free low-energy signals of new physics (NP).
- 4) Manifestation for charm quark existence came from low energy kaon oscillation experiments. Similar to this, one can hope that oscillations of charmed hadrons can provide hints of what is happening at the TeV scale.

The meson $D_{(s)}$, which contains one heavy charm quark c and one light quark, is placed in the heavy mesons category. The heavy charmed meson can decay into the axial vector mesons by emitting a pair of leptons $\ell\nu$ through weak interaction. In quark level, this process is induced by the semileptonic decay of charm quark $c \rightarrow q\ell\nu$, where $q = d, s$. This light quark d or s is bound with the initial light quark in the charmed meson by strong interaction to form an axial vector meson. It should be noted that another category of charmed meson decays can be fulfilled by the flavor changing neutral currents (FCNC) at tree level in SM via the $c \rightarrow u\ell^+\ell^-$ transition such as $D \rightarrow \pi\ell^+\ell^-$, $D \rightarrow \rho\ell^+\ell^-$, $D \rightarrow \pi\gamma$ and $D \rightarrow \rho\gamma$ decays (for more detailed, see [2]). Analyzing the semileptonic decays of the charmed $D_{(s)}$ meson is important for determination of the Cabibbo-Kabayashi-Maskawa (CKM) matrix elements, checking the standard model and also calculation of the leptonic decay constants of the initial and final meson states.

Nonperturbative effects of semileptonic decays can be parameterized by transition form factors. Considering the transition form factors for the semileptonic decays of mesons has two-fold importance:

- A number of the physical observables such as decay width and branching ratio, in addition some parameters of the SM can be investigated using these form factors.
- The factorization of amplitudes in the nonleptonic two-body decays can be fulfilled in terms of the transition form factors.

The form factors are calculated by various methods. Each method is more powerful than other methods in a certain region of the transferred momentum square q^2 . In the region $q^2 \rightarrow 0$ where the momentum of the outgoing meson is high, the large energy effective theory (LEET) can be used for determining of the form factors. In the region of large momentum transfer ($q^2 \rightarrow q_{max}^2$), the lattice QCD (LQCD) can be used. In $q^2 = q_{max}^2$, the Form factors can be calculated within the heavy-light chiral perturbation theory ($HL_\chi PT$), that is based on the heavy quark effective theory (HQET). Calculations within $HL_\chi PT$ can also be completed by calculations in the frame work of the heavy-light chiral quark model ($HL_\chi QM$). Corrections via the heavy quark symmetry are of the order $\mathcal{O}(1/m_c)$, which will be larger in the D sector than in the B sector [3].

* e-mail: samira.momeni@ph.iut.ac.ir

† e-mail: rezakhosravi @ cc.iut.ac.ir

A particularly approach to heavy-to-light transitions is offered by QCD sum rules on the light-cone. The LCSR approach combine operator product expansion (OPE) on the light-cone with QCD sum rule techniques in the region that q^2 is near zero. In this approach, the nonperturbative hadronic matrix elements are described by the light-cone distribution amplitudes (LCDAs) of increasing twist instead of the vacuum condensates (for more details, see Refs. [4–8]).

The form factors of the semileptonic decays of charmed meson $D_{(s)}$ to scalar, pseudoscalar or vector mesons have been estimated by various approaches. The form factors of the semileptonic decays $D^+ \rightarrow (D^0, \rho^0, \omega, \eta, \eta')\ell^+\nu$ and $D_s^+ \rightarrow (D^0, \phi, K^0, K^{*0}, \eta, \eta')\ell^+\nu$ have been computed in the framework of the covariant confined quark model (CCQM) [9, 10]. Both the vector and scalar form factors of $D \rightarrow K\ell\nu$ decay have been determined from the experimental measurements [11]. In Ref. [12–14], the $D \rightarrow \pi(K, \rho)\ell\nu$ decays have been studied by the LCSR approach. The semileptonic processes $D \rightarrow \pi, \rho, K$ and K^* have been investigated by the HQET in Ref. [15], while the form factors of the $D \rightarrow \pi(K, K^*)\ell\nu$ transitions have been evaluated by the LQCD method in Ref. [16–18]. The semileptonic decays $D_{(s)} \rightarrow f_0(K_0^*)\ell\nu$, $D_{(s)} \rightarrow \pi(K)\ell\nu$, and $D_{(s)} \rightarrow K^*(\rho, \phi)\ell\nu$ have been studied in the framework of the three-point QCD sum rules (3PSR) [19–25]. For the axial vector meson, as the final state in D meson decays, the $D_q \rightarrow K_1\ell\nu$ ($q = u, d, s$) and $D \rightarrow a_1, f_1(1285), f_1(1420)$ transitions have been analyzed by the 3PSR approach [26, 27].

The main purpose of this paper is the form factor investigation for the semileptonic decays of $D_{(s)}$ meson to the axial vector mesons such as: $D^0 \rightarrow a_1^-(b_1^-)\ell^+\nu$, $D^+ \rightarrow a_1^0(b_1^0)\ell^+\nu$, $D_s^+ \rightarrow K_1^0\ell^+\nu$ as well as $D^+ \rightarrow K_1^0\ell^+\nu$ decays. The first three cases of these decays are described by $c \rightarrow d\ell\nu$ transition at quark level, while the latter is proceed by $c \rightarrow s\ell\nu$ transition. We plan to calculate the form factors of the aforementioned semileptonic decays up to the twist-3 DAs of the axial vector mesons in the framework of the LCSR. It should be noted that we keep out all terms including m_A/m_c (m_A stands for the axial vector mass) in the expansion of the two-particle DAs of the axial vector mesons since their masses are comparable to quark mass m_c . We compare our results for the transition form factors of the semileptonic decays with predictions obtained from other methods. Using the computed form factors, the branching ratios of the nonleptonic $D^0 \rightarrow K_1^-(1270)\pi^+$, $D^0 \rightarrow K_1^-(1400)\pi^+$, $D^+ \rightarrow K_1^0(1270)\pi^+$ and $D^+ \rightarrow K_1^0(1400)\pi^+$ decays are considered. A comparison is made between our values for the branching ratios of the aforementioned nonleptonic decays with results obtained from other approaches as well as existing experimental values.

The physical states of $K_1(1270)$ and $K_1(1400)$ mesons are considered as a mixture of two $|K_{1A}\rangle$ and $|K_{1B}\rangle$ states and can be parameterized in terms of a mixing angle θ_K , as follows [28]:

$$\begin{aligned} |K_1(1270)\rangle &= \sin\theta_K|K_{1A}\rangle + \cos\theta_K|K_{1B}\rangle, \\ |K_1(1400)\rangle &= \cos\theta_K|K_{1A}\rangle - \sin\theta_K|K_{1B}\rangle, \end{aligned} \quad (1)$$

where $|K_{1A}\rangle$ and $|K_{1B}\rangle$ have different masses and decay constants. Also, the mixing angle θ_K can be determined by the experimental data. There are various approaches to estimate the mixing angle. The result $35^\circ \leq |\theta_K| \leq 55^\circ$ was found in Ref. [29], while two possible solutions were obtained as $|\theta_K| \approx 33^\circ \vee 57^\circ$ in Ref. [30] and as $|\theta_K| \approx 37^\circ \vee 58^\circ$ in Ref. [31]. A new window for the value of θ_K is estimated from the results of $B \rightarrow K_1(1270)\gamma$ and $\tau \rightarrow K_1(1270)\nu_\tau$ data as [32]

$$\theta_K = -(34 \pm 13)^\circ. \quad (2)$$

Sofar this value is used in Refs. [33–38]. In this study, we also use the result of $\theta_K = -(34 \pm 13)^\circ$.

The paper is organized as follows: In Sec. II, by using the LCSR method, the form factors for the semileptonic decays of D to the axial vector mesons are derived. In Sec. III, we present our numerical analysis for the form factors and determine the branching ratio values of the semileptonic and nonleptonic decays. A comparison is also made between our results and the predictions of other methods in this section.

II. TRANSITION FORM FACTORS IN THE LCSR

To calculate the form factors of the semileptonic transition of D^0 to the axial vector meson a_1^- ($D^0 \rightarrow a_1^-\ell^+\nu$) in the LCSR method, we consider the following correlation function as

$$\Pi_\mu(p, p') = i \int d^4x e^{iqx} \langle a_1^-(p', \varepsilon) | \mathcal{T} \{ \bar{d}(x) \gamma_\mu (1 - \gamma_5) c(x) j_{D^0}^\dagger(0) \} | 0 \rangle, \quad (3)$$

in this correlation function, $q = p - p'$, where p and p' are the four-momentum of the initial and final meson states, respectively. In addition, $j_{D^0} = i\bar{u}\gamma_5 c$ is known as the interpolating current of D^0 meson. Current $\bar{d}\gamma_\mu(1 - \gamma_5)c$ is the interaction current for semileptonic $D^0 \rightarrow a_1^-$ transition.

Following the general idea of the LCSR, the correlation function in Eq. (3) should be calculated in two different languages: 1) in terms of hadronic properties which we say the physical representation, and 2) quark and gluon degrees of freedom which is the theoretical side. Equating two sides and applying the Borel transformation to suppress the contribution of the higher states and continuum, we get sum rule expressions for the form factors. Let us first consider the physical representation of the correlator function.

To obtain the phenomenological or physical representation of the correlation function, a complete set of intermediate states with the same quantum numbers as the current J_{D^0} is inserted between two currents in Eq. (3). Isolating the pole mass term of the pseudoscalar D^0 meson and applying Fourier transformation, we get

$$\Pi_\mu(p', p) = \frac{\langle a_1^-(p', \varepsilon) | \bar{d} \gamma_\mu (1 - \gamma_5) c | D^0(p) \rangle \langle D^0(p) | \bar{c} i \gamma_5 u | 0 \rangle}{m_{D^0}^2 - p^2} + \text{higher states and continuum.} \quad (4)$$

The matrix element $\langle a_1^-(p', \varepsilon) | \bar{d} \gamma_\mu (1 - \gamma_5) c | D^0(p) \rangle$ is parameterized in terms of the form factors as follows:

$$\begin{aligned} \langle a_1^-(p', \varepsilon) | \bar{d} \gamma_\mu (1 - \gamma_5) c | D^0(p) \rangle = & i \frac{2A(q^2)}{m_{D^0} - m_{a_1^-}} \epsilon_{\mu\nu\alpha\beta} \varepsilon^{*\nu} p^\alpha p'^\beta - V_1(q^2) \varepsilon_\mu^* (m_{D^0} - m_{a_1^-}) \\ & + \frac{V_2(q^2)}{m_{D^0} - m_{a_1^-}} (\varepsilon^* \cdot q)(p + p')_\mu + \frac{(\varepsilon^* \cdot q) 2m_{a_1^-}}{q^2} q_\mu [V_3(q^2) - V_0(q^2)], \end{aligned} \quad (5)$$

where $m_{a_1^-}$ and ε_μ are the mass and the four-polarization vector of the axial vector meson a_1^- , respectively. In Eq. (5), $A(q^2)$ and $V_i(q^2)$ ($i = 0, \dots, 3$) are the transition form factors of the $D^0 \rightarrow a_1^- \ell^+ \nu$ decay. Form factor $V_3(0)$ can be written as a linear combination of $V_1(q^2)$ and $V_2(q^2)$ as

$$V_3(q^2) = \frac{m_{D^0} - m_{a_1^-}}{2m_{a_1^-}} V_1(q^2) - \frac{m_{D^0} + m_{a_1^-}}{2m_{a_1^-}} V_2(q^2), \quad (6)$$

with the condition $V_0(0) = V_3(0)$.

The second matrix element in Eq. (4) is expressed in the standard way as

$$\langle D^0(p) | \bar{c} i \gamma_5 u | 0 \rangle = \frac{f_{D^0} m_{D^0}^2}{m_c + m_d}, \quad (7)$$

where f_D is the D meson decay constant and $m_c(m_d)$ is the $c(d)$ quark mass. Using Eqs. (5) and (7) in Eq. (4), the phenomenological part of the correlation function is written in terms of the form factors and Lorentz structures as

$$\begin{aligned} \Pi_\mu = & -\frac{f_{D^0} m_{D^0}^2}{m_c + m_d} \frac{1}{p^2 - m_{D^0}^2} \left\{ i \frac{2A(q^2)}{m_{D^0} - m_{a_1^-}} \epsilon_{\mu\nu\alpha\beta} \varepsilon^{*\nu} p^\alpha p'^\beta - V_1(q^2) \varepsilon_\mu^* (m_{D^0} - m_{a_1^-}) \right. \\ & \left. + \frac{V_2(q^2)}{m_{D^0} - m_{a_1^-}} (\varepsilon^* \cdot q)(p + p')_\mu + \frac{(\varepsilon^* \cdot q) 2m_{a_1^-}}{q^2} q_\mu [V_3(q^2) - V_0(q^2)] \right\} + \frac{1}{\pi} \int_{s_0}^\infty \frac{\rho_\mu^h(s)}{s - p^2} ds, \end{aligned} \quad (8)$$

where ρ_μ^h is the spectral density of the higher resonances and continuum. This spectral density can be approximated by evoking the quark-hadron duality assumption as:

$$\rho_\mu^h(s) \simeq \rho_\mu^{QCD}(s) \theta(s - s_0), \quad (9)$$

$\rho_\mu^{QCD}(s)$ is the perturbative QCD spectral density investigated from the theoretical side of the correlation function. The threshold s_0 is chosen near the squared mass of the lowest D^0 meson state.

Now, the QCD or the theoretical part of the correlation function should be calculated. The calculation of the Π_μ in the region of large space-like momentum is based on the expansion of the \mathcal{T} -product of the interpolating and interaction currents near the light-cone. After contracting c and \bar{c} quark fields, we get

$$\Pi_\mu = \int d^4x e^{iqx} \langle a_1^-(p', \varepsilon) | \bar{d}(x) \gamma_\mu (1 - \gamma_5) S^c(x, 0) \gamma_5 u(0) | 0 \rangle, \quad (10)$$

where $S^c(x, 0)$ is the full propagator of the c quark in presence of the background gluon field as

$$\begin{aligned} S^c(x) = & \int \frac{d^4k}{(2\pi)^4} e^{-ikx} \frac{\not{k} + m_c}{k^2 - m_c^2} - g_s \int \frac{d^4k}{(2\pi)^4} e^{-ikx} \int_0^1 du \left[\frac{1}{2} \frac{\not{k} + m_c}{(m_c^2 - k^2)^2} G_{\mu\nu}(ux) \sigma^{\mu\nu} \right. \\ & \left. + \frac{1}{m_c^2 - k^2} u x_\mu G^{\mu\nu}(ux) \gamma_\nu \right]. \end{aligned} \quad (11)$$

The first term on the right-hand-side corresponds to the free quark propagator, $G_{\mu\nu}$ is the gluon field strength tensor and g_s is the strong coupling constant. In the present work, contributions with two gluons as well as four quark operators are neglected because their contributions are small. For obtaining the theoretical part of the correlation function, the Fierz rearrangement is used. For this aim, the combination of $\Gamma^i \Gamma_i$ is inserted before $u(0)$ in Eq. (10), where Γ_i is the full set of the Dirac matrices, $\Gamma_i = (I, \gamma_5, \gamma_\mu, \gamma_\mu \gamma_5, \sigma_{\mu\nu})$. After rearrangement the quantum fields and matrices appearing in the correlation function, in addition considering all terms of the full propagator $S^c(x, 0)$, it turns into two parts including a matrix trace and a matrix element of non-local operators between a_1^- meson and vacuum state, i.e., $\langle a_1^- | \bar{d}(x) \Gamma_i u(0) | 0 \rangle$ and $\langle a_1^- | \bar{d}(x) \Gamma_i G_{\mu\nu} u(0) | 0 \rangle$. In the LCSR approach the non-zero matrix elements, called the LCDAs, are defined in terms of twist functions. For instance, two-particle DA $\langle a_1^-(p', \varepsilon) | \bar{d}_\alpha(x) u_\delta(0) | 0 \rangle$ is presented as [39]:

$$\begin{aligned} \langle a_1^-(p', \varepsilon) | \bar{d}_\alpha(x) u_\delta(0) | 0 \rangle = & -\frac{i}{4} \int_0^1 du e^{iup' \cdot x} \left\{ f_{a_1^-} m_{a_1^-} \left[\not{p}' \gamma_5 \frac{\varepsilon^* \cdot x}{p' \cdot x} \Phi_{\parallel}(u) + \left(\not{\varepsilon}^* - \not{p}' \frac{\varepsilon^* \cdot x}{p' \cdot x} \right) \gamma_5 g_{\perp}^{(a)}(u) \right. \right. \\ & - \not{x} \gamma_5 \frac{\varepsilon^* \cdot x}{2(p' \cdot x)^2} m_{a_1^-}^2 \phi_b(u) + \epsilon_{\mu\nu\rho\sigma} \varepsilon^{*\nu} p'^\rho x^\sigma \gamma^\mu \frac{g_{\perp}^{(v)}(u)}{4} \left. \right] \\ & + f_A \left[\frac{1}{2} (\not{p}' \not{\varepsilon}^* - \not{\varepsilon}^* \not{p}') \gamma_5 \Phi_{\perp}(u) - \frac{1}{2} (\not{p}' \not{x} - \not{x} \not{p}') \gamma_5 \frac{\varepsilon^* \cdot x}{(p' \cdot x)^2} m_{a_1^-}^2 \bar{h}_{\parallel}^{(t)}(u) \right. \\ & \left. \left. + i(\varepsilon^* \cdot x) m_{a_1^-}^2 \gamma_5 \frac{h_{\parallel}^{(p)}(u)}{2} \right] \right\}_{\delta\alpha}, \end{aligned} \quad (12)$$

where Φ_{\parallel} , Φ_{\perp} are twist-2, $g_{\perp}^{(a)}$, $g_{\perp}^{(v)}$, $h_{\parallel}^{(t)}$ and $h_{\parallel}^{(p)}$ are twist-3 functions. For $x^2 \neq 0$, we have

$$\begin{aligned} \phi_b(u) &= \Phi_{\parallel} - 2g_{\perp}^{(a)}(u), \\ \bar{h}_{\parallel}^{(t)} &= h_{\parallel}^{(t)} - \frac{1}{2} \Phi_{\perp}(u). \end{aligned}$$

We should keep out all terms of the two-parton LCDA in Eq. (12) in our calculations, since the mass of the axial vector meson a_1^- is comparable to the charm quark mass. The explicit expressions for the relevant two- and three-parton LCDAs and definitions for the above mentioned twist functions are collected in Appendix A.

Using the LCDAs and after some straightforward calculations, the correlation function in theoretical side appears as an integral expression that made up of the twist functions and Lorentz structures.

To equate the coefficients of the corresponding Lorentz structures from both phenomenological and theoretical sides of the correlation function and apply Borel transform with respect to the variable p^2 as

$$B_{p^2}(M^2) \frac{1}{(p^2 - m_{D^0}^2)^n} = \frac{(-1)^n e^{-\frac{m_{D^0}^2}{M^2}}}{\Gamma(n) (M^2)^n}, \quad (13)$$

in order to suppress the higher states and continuum contributions, one can obtain the transition form factors of the $D^0 \rightarrow a_1^- \ell^+ \nu$ decay in the frame work of the LCSR. For instance, the form factor $A(q^2)$ is calculated as

$$A(q^2) = -\frac{m_c(m_{D^0} - m_{a_1^-}) f_{a_1^-}}{m_{D^0}^2 f_{D^0}} e^{m_{D^0}^2/M^2} \int_{u_0}^1 du e^{s(u)} \left[\frac{9 f_{a_1^-}^{\perp}}{f_{a_1^-}} \frac{\Phi_{\perp}(u)}{u} + \frac{32 f_{a_1^-}^{\perp}}{f_{a_1^-}} \frac{m_{a_1^-}^2}{M^2} \frac{\bar{h}_{\parallel}^{(t)(ii)}(u)}{u} + \frac{m_c m_{a_1^-}}{2 M^2} \frac{g_{\perp}^{(v)}(u)}{u^2} \right], \quad (14)$$

where u_0 is the function of s_0 , the continuum threshold of D^0 meson, as

$$u_0(s_0) = \frac{1}{2m_{a_1^-}^2} \left[\sqrt{(s_0 - m_{a_1^-}^2 - q^2)^2 + 4m_{a_1^-}^2(m_c^2 - q^2)} - (s_0 - m_{a_1^-}^2 - q^2) \right]. \quad (15)$$

The explicit expressions for the other form factors are presented in Appendix B.

Following the previous steps in this section, phrases similar to Eq. (14) and Appendix B can be obtained for the transition form factors of $D^0 \rightarrow b_1^- \ell^+ \nu$, $D^+ \rightarrow a_1^0(b_1^0) \ell^+ \nu$, $D_s^+ \rightarrow K_1^0 \ell^+ \nu$ as well as $D^+ \rightarrow K_1^0 \ell^+ \nu$ decays via the LCSR approach.

III. NUMERICAL ANALYSIS

We present our numerical analysis for the form factors and branching ratio values of the semileptonic $D_{(s)} \rightarrow A \ell^+ \nu$, where $A = a_1, b_1, K_1(1270, 1400)$, and the nonleptonic $D \rightarrow K_1(1270, 1400)\pi$ decays in two subsections. First, the transition form factors and branching ratio values of the semileptonic $D^+ \rightarrow a_1^0(b_1^0, K_1^0)\ell^+\nu$, $D^0 \rightarrow a_1^-(b_1^-)\ell^+\nu$, and $D_s^+ \rightarrow K_1^0\ell^+\nu$ decays are analyzed. In the next subsection, using these form factors, the branching ratio values are calculated for the nonleptonic $D^0 \rightarrow K_1^-(1270)\pi^+$, $D^0 \rightarrow K_1^-(1400)\pi^+$, $D^+ \rightarrow K_1^0(1270)\pi^+$ and $D^+ \rightarrow K_1^0(1400)\pi^+$ decays via the factorization method. For a better analysis, a comparison is made between our results and predictions of the other methods and the experimental values.

In this work, masses are taken in GeV as $m_c = 1.28 \pm 0.03$, $m_D = 1.86$ and $m_{D_s} = 1.96$ [40]. We use the results of the QCD sum rules for decay constants of D and D_s mesons, rather than the actual value of them, as $f_D = 210 \pm 12$ MeV and $f_{D_s} = 246 \pm 8$ MeV [41]; in this way radiative correction will be canceled. Masses and decay constant values for the axial vector mesons are collected in Table I. We can take $f_A = f_A^\perp$ at energy scale $\mu = 1$ GeV [39]. All of the decay constant values for the axial vector mesons in Table I, and also masses for two K_{1A} and K_{1B} states are estimated from the LCSR [39].

TABLE I: Masses and decay constants for axial vector mesons and two states K_{1A} and K_{1B} [39, 40].

Mass	m_{a_1}	m_{b_1}	$m_{K_{1A}}$	$m_{K_{1B}}$
Value (GeV)	1.23 ± 0.40	1.23 ± 0.32	1.31 ± 0.06	1.34 ± 0.08
Decay Constant	f_{a_1}	f_{b_1}	$f_{K_{1A}}$	$f_{K_{1B}}$
Value (MeV)	238 ± 10	180 ± 8	250 ± 13	190 ± 10

It should be noted that the decay constants of $K_1(1270)$ and $K_1(1400)$ mesons are written in terms of $f_{K_{1A}}$ and $f_{K_{1B}}$ as [39]:

$$\begin{aligned}
 f_{K_1(1270)} &= \sin \theta_K \frac{m_{K_{1A}}}{m_{K_1(1270)}} f_{K_{1A}} + \cos \theta_K \frac{m_{K_{1B}}}{m_{K_1(1270)}} a_0^{\parallel, K_{1B}} f_{K_{1B}}, \\
 f_{K_1(1400)} &= \cos \theta_K \frac{m_{K_{1A}}}{m_{K_1(1400)}} f_{K_{1A}} - \sin \theta_K \frac{m_{K_{1B}}}{m_{K_1(1400)}} a_0^{\parallel, K_{1B}} f_{K_{1B}},
 \end{aligned} \tag{16}$$

where $a_0^{\parallel, K_{1B}}$ is G-parity invariant Gegenbauer moment for K_{1B} state.

A. Analysis of semileptonic decays

From the formulas presented in Eq. (14) and Appendix B for the form factors of the semileptonic $D^0 \rightarrow a_1^- \ell^+ \nu$ decays, it is easily known that they contain two free parameters M^2 and s_0 , which are the Borel mass-square and the continuum threshold of D^0 meson, respectively. M^2 and s_0 are not physical quantities; therefore, the form factors as physical quantities should be independent of them. The Borel parameter must be large enough to suppress the contribution of higher states. On the other hand, it should be small enough to show the effect of twist functions.

For instance in Fig. 1, the dependence of the $D^0 \rightarrow a_1^-$ form factors is displaced with respect to M^2 , at $q^2 = 0$, for three values of $s_0 = 6.8, 7$ and 7.2 GeV² with dot, solid and dash-dot lines, respectively. In this figure, shaded interval shows the proper region of the Borel parameter for each transition form factor of the semileptonic $D^0 \rightarrow a_1^-$ decay. As can be seen in Fig. 1, the form factors A , V_1 , V_2 and V_0 of the $D^0 \rightarrow a_1^-$ transition, obtained from the sum rules in $s_0 = 7$ GeV², can be stable within the Borel mass intervals $5 \text{ GeV}^2 < M^2 < 8 \text{ GeV}^2$, $8 \text{ GeV}^2 < M^2 < 10 \text{ GeV}^2$, and $6 \text{ GeV}^2 < M^2 < 9 \text{ GeV}^2$ and $9 \text{ GeV}^2 < M^2 < 11 \text{ GeV}^2$, respectively. From now on, we get the continuum threshold of $D_{(s)}$ meson for all decays equal to $s_0 = 7$ GeV² in our calculations.

Having all the required parameters, we can estimate the form factors for each aforementioned semileptonic decay. The LCSR predictions for the form factors are valid in half of the physical region $m_\ell^2 \leq q^2 \leq (m_{D_{(s)}} - m_A)^2$, nearly, and then these quantities are truncated at some points. In order to extend our results to the full physical region, we look for parametrization of the form factors in such a way that in the validity region of the LCSR, this parametrization

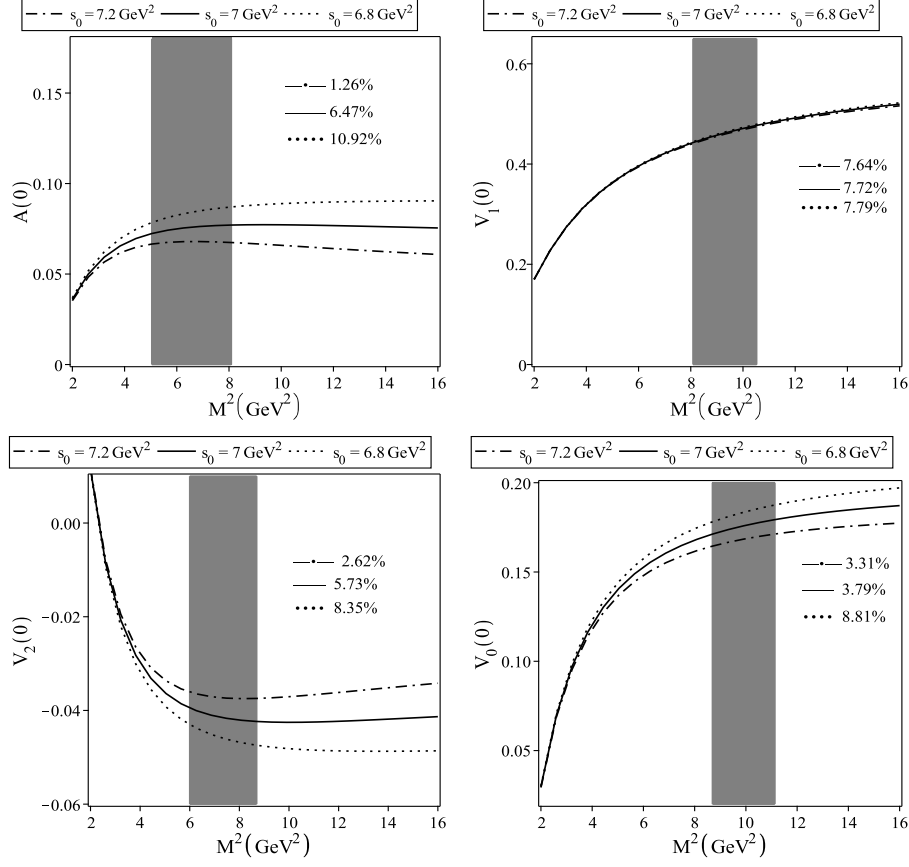


FIG. 1: $D^0 \rightarrow a_1^-$ transition form factors as functions of M^2 at $q^2 = 0$. The dot, solid and dot-dashed lines correspond to $s_0 = 6.8, 7$ and 7.2 GeV^2 , respectively

coincides with the sum rules predictions. We use the following fit functions of the form factors with respect to q^2 as:

$$F^{(1)}(q^2) = \frac{1}{1 - q^2/m_{D(s)}^2} \sum_{l=0}^2 b_l \left[z^l + (-1)^l \frac{l}{3} z^4 \right], \quad (17)$$

$$F^{(2)}(q^2) = \frac{F(0)}{1 - \alpha (q^2/m_{D(s)}^2) + \beta (q^2/m_{D(s)}^2)^2}, \quad (18)$$

$$F^{(3)}(q^2) = \frac{c_1}{1 - q^2/m_{D^*}^2} + \frac{c_2}{(1 - q^2/m_{D^*}^2)^2}, \quad (19)$$

$$F^{(4)}(q^2) = \frac{r_1}{1 - q^2/m_{D^*}^2} + \frac{r_2}{1 - q^2/m_{\text{fit}}^2}, \quad (20)$$

where $z = \frac{\sqrt{t_+ - q^2} - \sqrt{t_+ - t_0}}{\sqrt{t_+ - q^2} + \sqrt{t_+ - t_0}}$, $t_+ = (m_{D(s)} + m_A)^2$ and $t_0 = (m_{D(s)} + m_A)(\sqrt{m_{D(s)}} - \sqrt{m_A})^2$ [42].

Tables II, III, IV and V show the values of $[b_0, b_1, b_2]$, $[F(0), \alpha, \beta]$, $[c_1, c_2]$, and also $[r_1, r_2, m_{\text{fit}}]$ respectively, for the form factors of the semileptonic decays.

The dependence of the form factors, $A, V_i (i = 0, 1, 2)$, for $D^0 \rightarrow a_1^-$ transition on q^2 are given in Fig. 2. In this figure the blue, red, purple and yellow lines show the results for $F^{(1)}, F^{(2)}, F^{(3)}$ and $F^{(4)}$ fit functions, respectively. According to the Fig. 2, the form factors obtained for the four fit functions are in a good agreement with each other and there is no significant change in their dependence on q^2 .

The semileptonic $D_{(s)} \rightarrow K_{1A} \ell \nu$, $D_{(s)} \rightarrow K_{1B} \ell \nu$, $D^0 \rightarrow a_1^- \ell^+ \nu$ and $D^+ \rightarrow a_1^0 \ell^+ \nu$ decays have been studied via the 3PSR and LFQM approaches [26, 27, 43]. In Tables VI and VII, we compare our results for the form factors of the aforementioned decays at the zero transferred momentum square $q^2 = 0$ with the the 3PSR and LFQM values which have been rescaled according to the form factor definition in Eq. (5). In these tables, the errors of the LCSR

TABLE II: Values of b_0 , b_1 and b_2 related to $F^{(1)}(q^2)$ for the fitted form factors of $D_{(s)} \rightarrow a_1, b_1, K_{1A}$ and K_{1B} transitions.

Form factor	b_0	b_1	b_2	Form factor	b_0	b_1	b_2
$A^{D^0 \rightarrow a_1^-}$	0.08	0.45	19.42	$A^{D^0 \rightarrow b_1^-}$	-0.39	-2.75	25.99
$V_1^{D^0 \rightarrow a_1^-}$	0.40	3.49	6.64	$V_1^{D^0 \rightarrow b_1^-}$	-0.22	0.07	36.37
$V_2^{D^0 \rightarrow a_1^-}$	-0.03	-0.74	-1.21	$V_2^{D^0 \rightarrow b_1^-}$	0.19	2.72	23.43
$V_0^{D^0 \rightarrow a_1^-}$	0.14	0.99	-9.16	$V_0^{D^0 \rightarrow b_1^-}$	-0.25	-10.98	-64.47
$A^{D^+ \rightarrow a_1^0}$	0.05	0.27	12.35	$A^{D^+ \rightarrow b_1^0}$	-0.26	-1.94	20.47
$V_1^{D^+ \rightarrow a_1^0}$	0.27	2.38	4.01	$V_1^{D^+ \rightarrow b_1^0}$	-0.16	0.09	25.63
$V_2^{D^+ \rightarrow a_1^0}$	-0.03	-0.56	-0.71	$V_2^{D^+ \rightarrow b_1^0}$	0.13	1.96	16.72
$V_0^{D^+ \rightarrow a_1^0}$	0.69	0.71	-5.63	$V_0^{D^+ \rightarrow b_1^0}$	-0.23	0.49	217.83
$A^{D \rightarrow K_{1A}}$	0.06	0.49	18.92	$A^{D \rightarrow K_{1B}}$	-0.51	-3.65	39.48
$V_1^{D \rightarrow K_{1A}}$	0.35	3.40	5.02	$V_1^{D \rightarrow K_{1B}}$	-0.29	0.14	66.82
$V_2^{D \rightarrow K_{1A}}$	-0.02	-0.59	0.38	$V_2^{D \rightarrow K_{1B}}$	0.29	5.31	49.19
$V_0^{D \rightarrow K_{1A}}$	0.16	2.82	-116.30	$V_0^{D \rightarrow K_{1B}}$	0.36	-13.69	-119.16
$A^{D_s \rightarrow K_{1A}}$	0.06	0.39	18.73	$A^{D_s \rightarrow K_{1B}}$	-0.47	-3.11	37.49
$V_1^{D_s \rightarrow K_{1A}}$	0.32	2.83	3.96	$V_1^{D_s \rightarrow K_{1B}}$	-0.27	0.35	56.71
$V_2^{D_s \rightarrow K_{1A}}$	-0.01	-0.40	-0.64	$V_2^{D_s \rightarrow K_{1B}}$	0.26	4.61	45.89
$V_0^{D_s \rightarrow K_{1A}}$	0.09	0.54	-10.98	$V_0^{D_s \rightarrow K_{1B}}$	-0.33	-16.04	-166.56

TABLE III: Values of $F(0)$, α and β connected to $F^{(2)}(q^2)$ for the fitted form factors of $D_{(s)} \rightarrow a_1, b_1, K_{1A}$ and K_{1B} transitions.

Form factor	$F(0)$	α	β	Form factor	$F(0)$	α	β
$A^{D^0 \rightarrow a_1^-}$	0.08	0.25	-2.17	$A^{D^0 \rightarrow b_1^-}$	-0.41	0.45	0.40
$V_1^{D^0 \rightarrow a_1^-}$	0.42	0.23	-0.18	$V_1^{D^0 \rightarrow b_1^-}$	-0.22	1.20	1.47
$V_2^{D^0 \rightarrow a_1^-}$	-0.04	-0.72	1.54	$V_2^{D^0 \rightarrow b_1^-}$	0.21	-0.31	-0.38
$V_0^{D^0 \rightarrow a_1^-}$	0.15	0.46	0.36	$V_0^{D^0 \rightarrow b_1^-}$	-0.32	-2.30	9.12
$A^{D^+ \rightarrow a_1^0}$	0.05	0.26	-2.21	$A^{D^+ \rightarrow b_1^0}$	-0.28	0.44	0.49
$V_1^{D^+ \rightarrow a_1^0}$	0.29	0.24	-0.17	$V_1^{D^+ \rightarrow b_1^0}$	-0.16	1.22	1.45
$V_2^{D^+ \rightarrow a_1^0}$	-0.03	-0.72	1.61	$V_2^{D^+ \rightarrow b_1^0}$	0.15	-0.32	-0.36
$V_0^{D^+ \rightarrow a_1^0}$	0.10	0.41	0.34	$V_0^{D^+ \rightarrow b_1^0}$	-0.23	-2.15	8.47
$A^{D \rightarrow K_{1A}}$	0.07	0.21	-2.14	$A^{D \rightarrow K_{1B}}$	-0.53	0.46	0.38
$V_1^{D \rightarrow K_{1A}}$	0.37	0.20	-0.13	$V_1^{D \rightarrow K_{1B}}$	-0.29	1.17	1.72
$V_2^{D \rightarrow K_{1A}}$	-0.03	-0.70	1.81	$V_2^{D \rightarrow K_{1B}}$	0.31	-0.49	-0.21
$V_0^{D \rightarrow K_{1A}}$	0.11	0.44	0.61	$V_0^{D \rightarrow K_{1B}}$	-0.42	-2.33	9.24
$A^{D_s \rightarrow K_{1A}}$	0.07	0.25	-2.34	$A^{D_s \rightarrow K_{1B}}$	-0.49	0.50	0.44
$V_1^{D_s \rightarrow K_{1A}}$	0.34	0.24	-0.15	$V_1^{D_s \rightarrow K_{1B}}$	-0.27	1.28	1.80
$V_2^{D_s \rightarrow K_{1A}}$	-0.02	-0.84	1.92	$V_2^{D_s \rightarrow K_{1B}}$	0.29	-0.53	-0.24
$V_0^{D_s \rightarrow K_{1A}}$	0.10	0.61	0.72	$V_0^{D_s \rightarrow K_{1B}}$	-0.41	-2.37	9.92

values are estimated by the variation of the Borel parameter M^2 and variation of the LCDAs parameters. The main uncertainty comes from the parameters of twist-2 LCDAs.

The form factor $A(q^2)$ at $q^2 = 0$ is related to the strong coupling constant $g_{DD^*a_1}$ as

$$A(0) = \frac{f_{D^*}(m_D - m_{a_1})}{2m_{D^*}} g_{DD^*a_1}. \quad (21)$$

Considering $f_{D^*} = (0.23 \pm 0.02)\text{GeV}$, the value of $g_{DD^*a_1}$ is evaluated to be $(2.21 \pm 1.38)\text{GeV}^{-1}$.

Now, we study the differential decay widths $d\Gamma_L/dq^2$ and $d\Gamma_\pm/dq^2$ of the semileptonic decays $D_{(s)}$ to axial vector

TABLE IV: Values of c_1 and c_2 connected to $F^{(3)}(q^2)$ for the fitted form factors of $D_{(s)} \rightarrow a_1, b_1, K_{1A}$ and K_{1B} transitions.

Form factor	c_1	c_2	Form factor	c_1	c_2
$A^{D^0 \rightarrow a_1^-}$	0.12	-0.04	$A^{D^0 \rightarrow b_1^-}$	-0.63	0.22
$V_1^{D^0 \rightarrow a_1^-}$	0.72	-0.30	$V_1^{D^0 \rightarrow b_1^-}$	-0.19	-0.02
$V_2^{D^0 \rightarrow a_1^-}$	-0.10	0.06	$V_2^{D^0 \rightarrow b_1^-}$	0.45	-0.24
$V_0^{D^0 \rightarrow a_1^-}$	0.23	-0.08	$V_0^{D^0 \rightarrow b_1^-}$	-1.30	0.98
$A^{D^+ \rightarrow a_1^0}$	0.07	-0.02	$A^{D^+ \rightarrow b_1^0}$	-0.43	0.15
$V_1^{D^+ \rightarrow a_1^0}$	0.49	-0.20	$V_1^{D^+ \rightarrow b_1^0}$	-0.13	-0.02
$V_2^{D^+ \rightarrow a_1^0}$	-0.07	0.04	$V_2^{D^+ \rightarrow b_1^0}$	0.32	-0.18
$V_0^{D^+ \rightarrow a_1^0}$	0.15	-0.05	$V_0^{D^+ \rightarrow b_1^0}$	-0.07	-0.15
$A^{D \rightarrow K_{1A}}$	0.11	-0.04	$A^{D \rightarrow K_{1B}}$	-0.81	0.28
$V_1^{D \rightarrow K_{1A}}$	0.65	-0.28	$V_1^{D \rightarrow K_{1B}}$	-0.26	-0.02
$V_2^{D \rightarrow K_{1A}}$	-0.07	0.04	$V_2^{D \rightarrow K_{1B}}$	0.74	-0.43
$V_0^{D \rightarrow K_{1A}}$	0.17	-0.06	$V_0^{D \rightarrow K_{1B}}$	0.01	-0.43
$A^{D_s \rightarrow K_{1A}}$	0.11	-0.04	$A^{D_s \rightarrow K_{1B}}$	-0.73	0.24
$V_1^{D_s \rightarrow K_{1A}}$	0.58	-0.24	$V_1^{D_s \rightarrow K_{1B}}$	-0.21	-0.05
$V_2^{D_s \rightarrow K_{1A}}$	-0.05	0.03	$V_2^{D_s \rightarrow K_{1B}}$	0.69	-0.40
$V_0^{D_s \rightarrow K_{1A}}$	0.14	-0.04	$V_0^{D_s \rightarrow K_{1B}}$	-1.82	1.41

TABLE V: Values of r_1 , r_2 and m_{fit} connected to $F^{(4)}(q^2)$ for the fitted form factors of $D_{(s)} \rightarrow a_1, b_1, K_{1A}$ and K_{1B} transitions.

Form factor	r_1	r_2	m_{fit}	Form factor	r_1	r_2	m_{fit}
$A^{D^0 \rightarrow a_1^-}$	1.34	-1.26	1.82	$A^{D^0 \rightarrow b_1^-}$	-1.86	1.45	1.73
$V_1^{D^0 \rightarrow a_1^-}$	3.82	-3.40	1.78	$V_1^{D^0 \rightarrow b_1^-}$	1.49	-1.71	1.84
$V_2^{D^0 \rightarrow a_1^-}$	-1.07	1.03	1.80	$V_2^{D^0 \rightarrow b_1^-}$	3.86	-3.65	1.79
$V_0^{D^0 \rightarrow a_1^-}$	0.77	-0.62	1.75	$V_0^{D^0 \rightarrow b_1^-}$	-17.34	17.02	1.80
$A^{D^+ \rightarrow a_1^0}$	0.91	-0.86	1.82	$A^{D^+ \rightarrow b_1^0}$	-1.71	0.89	1.71
$V_1^{D^+ \rightarrow a_1^0}$	2.52	-2.30	1.78	$V_1^{D^+ \rightarrow b_1^0}$	1.13	-1.29	1.84
$V_2^{D^+ \rightarrow a_1^0}$	-0.71	0.68	1.79	$V_2^{D^+ \rightarrow b_1^0}$	2.80	-2.65	1.80
$V_0^{D^+ \rightarrow a_1^0}$	0.62	-0.52	1.76	$V_0^{D^+ \rightarrow b_1^0}$	9.37	-9.60	1.84
$A^{D \rightarrow K_{1A}}$	0.93	-0.86	1.81	$A^{D \rightarrow K_{1B}}$	-2.04	1.51	1.70
$V_1^{D \rightarrow K_{1A}}$	2.91	-2.54	1.76	$V_1^{D \rightarrow K_{1B}}$	1.15	-1.44	1.84
$V_2^{D \rightarrow K_{1A}}$	-0.63	0.60	1.78	$V_2^{D \rightarrow K_{1B}}$	4.39	-4.08	1.76
$V_0^{D \rightarrow K_{1A}}$	0.26	-0.15	1.57	$V_0^{D \rightarrow K_{1B}}$	9.35	-9.77	1.82
$A^{D_s \rightarrow K_{1A}}$	1.18	-1.11	1.92	$A^{D_s \rightarrow K_{1B}}$	-1.42	0.93	1.74
$V_1^{D_s \rightarrow K_{1A}}$	2.85	-2.48	1.87	$V_1^{D_s \rightarrow K_{1B}}$	2.12	-2.39	1.93
$V_2^{D_s \rightarrow K_{1A}}$	-0.47	0.45	1.88	$V_2^{D_s \rightarrow K_{1B}}$	5.05	-4.76	1.88
$V_0^{D_s \rightarrow K_{1A}}$	0.13	-0.03	1.36	$V_0^{D_s \rightarrow K_{1B}}$	-20.99	20.58	1.89

mesons A , given as

$$\begin{aligned}
\frac{d\Gamma_L(D_{(s)} \rightarrow A\ell\nu)}{dq^2} &= \left(\frac{q^2 - m_l^2}{q^2}\right)^2 \frac{\sqrt{\lambda} G_F^2 |V_{cq'}|^2}{384 \pi^3 m_{D_{(s)}}^3} \times \frac{1}{q^2} \left\{ 3m_l^2 \lambda V_0^2(q^2) + (m_l^2 + 2q^2) \right. \\
&\quad \times \left| \frac{1}{2m_A} \left[(m_{D_{(s)}}^2 - m_A^2 - q^2)(m_{D_{(s)}} - m_A)V_1(q^2) - \frac{\lambda}{m_{D_{(s)}} - m_A} V_2(q^2) \right] \right|^2 \Big\}, \\
\frac{d\Gamma_{\pm}(D_{(s)} \rightarrow A\ell\nu)}{dq^2} &= \left(\frac{q^2 - m_l^2}{q^2}\right)^2 \frac{\sqrt{\lambda} G_F^2 |V_{cq'}|^2}{384 \pi^3 m_{D_{(s)}}^3} \times \left\{ (m_l^2 + 2q^2) \lambda \left| \frac{A(q^2)}{m_{D_{(s)}} - m_A} \mp \frac{(m_{D_{(s)}} - m_A)V_1(q^2)}{\sqrt{\lambda}} \right|^2 \right\},
\end{aligned}$$

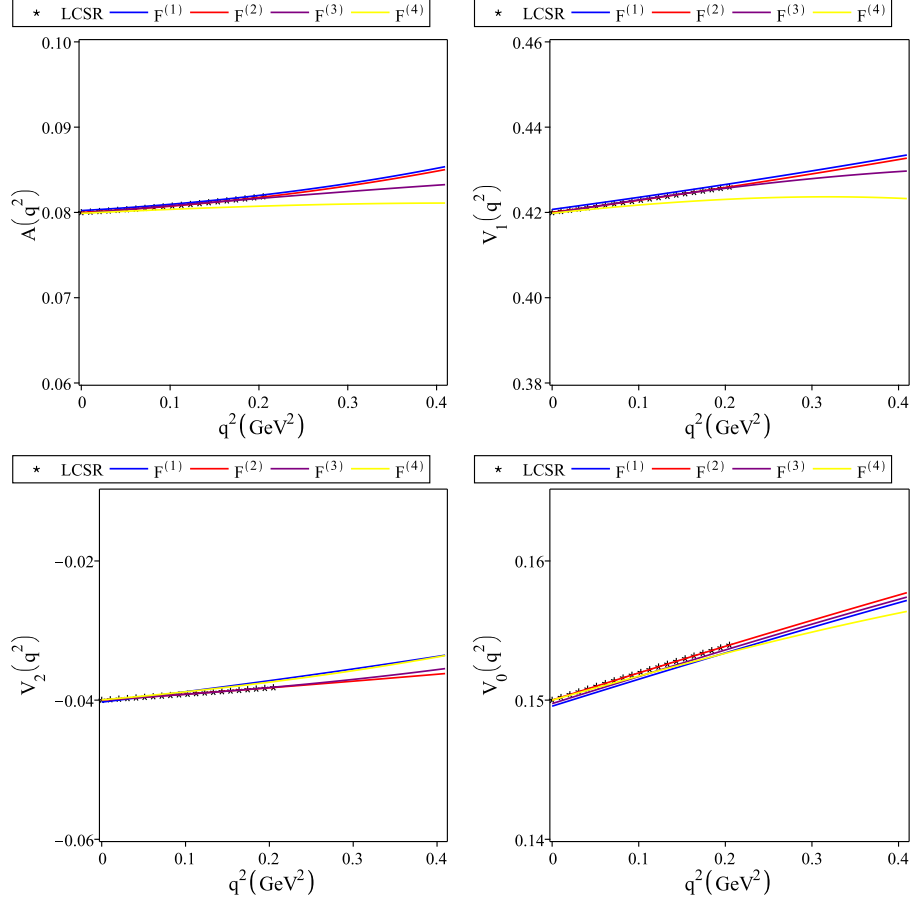


FIG. 2: Blue, red, purple and yellow lines show the form factors A , V_i ($i = 0, 1, 2$), obtained for $D^0 \rightarrow a_1^-$ transition on q^2 by using the $F^{(1)}$, $F^{(2)}$, $F^{(3)}$ and $F^{(4)}$ fit functions. Asterisks show the results of the LCSR.

TABLE VI: Transition form factors of $D_{(s)} \rightarrow K_{1A}(K_{1B})\ell\nu$ decays at $q^2 = 0$ in different approaches.

Decay	$D \rightarrow K_{1A}$		$D \rightarrow K_{1B}$		$D_s \rightarrow K_{1A}$		$D_s \rightarrow K_{1B}$	
Form factor	This work	3PSR [26]	This work	3PSR [26]	This work	3PSR [26]	This work	3PSR [26]
$A(0)$	0.06 ± 0.03	0.11	-0.47 ± 0.14	-0.75	0.05 ± 0.02	0.16	-0.40 ± 0.11	-0.84
$V_0(0)$	0.11 ± 0.03	0.04	-0.42 ± 0.14	-0.13	0.10 ± 0.04	0.03	-0.41 ± 0.12	-0.26
$V_1(0)$	0.32 ± 0.11	0.02	-0.26 ± 0.10	-0.16	0.28 ± 0.09	0.05	-0.22 ± 0.09	-0.30
$V_2(0)$	-0.03 ± 0.01	-0.01	0.29 ± 0.13	0.08	-0.01 ± 0.01	-0.02	0.24 ± 0.10	0.14

where $\lambda = m_{D(s)}^4 + m_A^4 + q^4 - 2m_A^2 m_{D(s)}^2 - 2q^2 m_{D(s)}^2 - 2q^2 m_A^2$. In these relations, for decays described by $c \rightarrow d(s)\ell\nu$ transition, $V_{cq'}$ becomes $V_{cd}(V_{cs})$. Also, $d\Gamma_L/dq^2$ and $d\Gamma_\pm/dq^2$ are the longitudinal and transverse components of the differential decay width, respectively. The total differential decay width can be written as

$$\frac{d\Gamma_{\text{tot}}(D_{(s)} \rightarrow A\ell\nu)}{dq^2} = \frac{d\Gamma_L(D_{(s)} \rightarrow A\ell\nu)}{dq^2} + \frac{d\Gamma_T(D_{(s)} \rightarrow A\ell\nu)}{dq^2}, \quad (22)$$

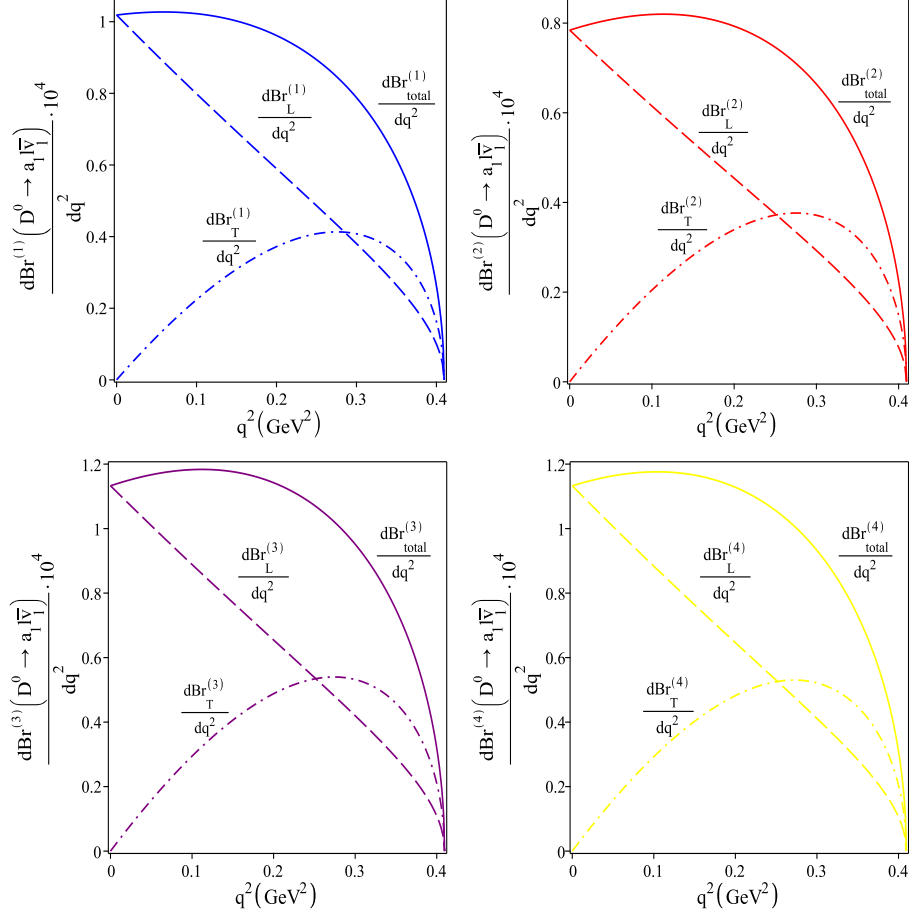
where

$$\frac{d\Gamma_T(D_{(s)} \rightarrow A\ell\nu)}{dq^2} = \frac{d\Gamma_+(D_{(s)} \rightarrow A\ell\nu)}{dq^2} + \frac{d\Gamma_-(D_{(s)} \rightarrow A\ell\nu)}{dq^2}. \quad (23)$$

We plot the differential branching ratios of $D^0 \rightarrow a_1^- \ell\nu$ with respect to q^2 in the physical region $m_\ell^2 \leq q^2 \leq (m_{D^0} - m_{a^-})^2$, in Fig. 3. In this figure, the solid, dash and dot-dashed lines depict the differential branching

TABLE VII: Transition form factors of $D^0 \rightarrow a_1^- \ell^+ \nu$ and $D^+ \rightarrow a_1^0 \ell^+ \nu$ at $q^2 = 0$ in various theoretical approaches.

Decay	$D^0 \rightarrow a_1^-$			$D^+ \rightarrow a_1^0$		
Form factor	This work	3PSR [27]	LFQM [43]	This work	3PSR [27]	LFQM [43]
$A(0)$	0.07 ± 0.05	0.09	0.20	0.04 ± 0.04	0.08	0.14
$V_0(0)$	0.15 ± 0.05	0.19	0.44	0.10 ± 0.03	0.12	0.30
$V_1(0)$	0.37 ± 0.11	0.77	1.54	0.26 ± 0.08	0.54	1.08
$V_2(0)$	-0.03 ± 0.02	-0.01	-0.06	-0.02 ± 0.01	-0.00	-0.04

FIG. 3: The differential branching ratio of $D \rightarrow a_1 \ell \nu$ decay as a function of q^2 . The solid, dash and dot-dashed lines depict the total, longitudinal and transverse differential branching ratio, respectively. Blue, red, purple and yellow plots show the results using the form factors fitted to $F^{(1)}$, $F^{(2)}$, $F^{(3)}$ and $F^{(4)}$.

ratios dBr_{tot}/dq^2 , dBr_L/dq^2 and dBr_T/dq^2 , respectively. Blue, red, purple and yellow plots show the results of the differential branching ratios using the form factors fitted to $F^{(1)}$, $F^{(2)}$, $F^{(3)}$ and $F^{(4)}$, respectively.

To calculate the branching ratio values of the semileptonic decays, we integrate Eq. (22) over q^2 in the whole physical region and use the total mean life-time $\tau_{D^0} = 0.41$, $\tau_{D^+} = 1.04$ and $\tau_{D_s} = 0.50$ ps [40]. To determine the branching ratio values of $D_{(s)} \rightarrow K_1(1270)\ell\nu$ and $D_{(s)} \rightarrow K_1(1400)\ell\nu$ decays, the transition form factors of them are needed. These form factors can be obtained in terms of the form factors of $D_{(s)} \rightarrow K_{1A}\ell\nu$ and $D_{(s)} \rightarrow K_{1B}\ell\nu$ decays with the help of the following transformations:

$$\begin{pmatrix} \langle K_1(1270) | \bar{s} \gamma_\mu (1 - \gamma_5) c | D \rangle \\ \langle K_1(1400) | \bar{s} \gamma_\mu (1 - \gamma_5) c | D \rangle \end{pmatrix} = \begin{pmatrix} \sin \theta_K & \cos \theta_K \\ \cos \theta_K & -\sin \theta_K \end{pmatrix} \begin{pmatrix} \langle K_{1A} | \bar{s} \gamma_\mu (1 - \gamma_5) c | D \rangle \\ \langle K_{1B} | \bar{s} \gamma_\mu (1 - \gamma_5) c | D \rangle \end{pmatrix}. \quad (24)$$

As previously mentioned, we use the result of $\theta_K = -(34 \pm 13)^\circ$.

The branching ratio values of the semileptonic decays $D_{(s)} \rightarrow A\ell\nu$ related to the form factors fitted to $F^{(i)}(i = 1, \dots, 4)$ are presented in Tables VIII- XI, respectively. In these tables, we compare our results with other approaches. The results presented for the branching ratio values of $D \rightarrow K_1(1270)\ell\nu$ and $D \rightarrow K_1(1400)\ell\nu$ decays in Tables

TABLE VIII: Branching ratio values of the semileptonic $D_{(s)} \rightarrow A\ell\nu$ related to fit function $F^{(1)}$.

Process	Br_T	Br_L	Br_{tot} (This work)	Br_{tot} [26]	Br_{tot} [27]	
$D^0 \rightarrow a_1^- \ell \nu$	$[1.16 \pm 0.15]$	2.36 ± 0.35	3.52 ± 0.50	--	$1.11^{+0.41}_{-0.34}$	$] \times 10^{-5}$
$D^+ \rightarrow a_1^0 \ell \nu$	$[1.52 \pm 0.19]$	3.05 ± 0.43	4.57 ± 0.62	--	$1.47^{+0.55}_{-0.44}$	$] \times 10^{-5}$
$D^0 \rightarrow b_1^- \ell \nu$	$[0.52 \pm 0.08]$	0.69 ± 0.10	1.21 ± 0.18	--	--	$] \times 10^{-5}$
$D^+ \rightarrow b_1^0 \ell \nu$	$[0.70 \pm 0.11]$	0.93 ± 0.15	1.63 ± 0.26	--	--	$] \times 10^{-5}$
$D^0 \rightarrow K_1^-(1270)\ell\nu$	$[2.89 \pm 0.05]$	5.20 ± 0.10	8.09 ± 0.15	5.34 ± 0.21	--	$] \times 10^{-3}$
$D^+ \rightarrow K_1^0(1270)\ell\nu$	$[7.77 \pm 0.12]$	10.82 ± 0.19	18.59 ± 0.31	14.07 ± 1.22	--	$] \times 10^{-3}$
$D_s^+ \rightarrow K_1^0(1270)\ell\nu$	$[0.88 \pm 0.03]$	1.27 ± 0.06	2.15 ± 0.09	1.25 ± 0.11	--	$] \times 10^{-3}$
$D^0 \rightarrow K_1^-(1400)\ell\nu$	$[0.32 \pm 0.03]$	0.43 ± 0.02	0.75 ± 0.03	0.85 ± 0.02	--	$] \times 10^{-3}$
$D^+ \rightarrow K_1^0(1400)\ell\nu$	$[0.37 \pm 0.03]$	0.56 ± 0.03	0.93 ± 0.06	1.27 ± 0.10	--	$] \times 10^{-3}$
$D_s^+ \rightarrow K_1^0(1400)\ell\nu$	$[0.05 \pm 0.01]$	0.08 ± 0.01	0.13 ± 0.02	0.14 ± 0.01	--	$] \times 10^{-3}$

TABLE IX: The same as Table VIII but related to fit function $F^{(2)}$.

Process	Br_T	Br_L	Br_{tot} (This work)	Br_{tot} [26]	Br_{tot} [27]	
$D^0 \rightarrow a_1^- \ell \nu$	$[1.06 \pm 0.14]$	1.79 ± 0.27	2.85 ± 0.41	--	$1.11^{+0.41}_{-0.34}$	$] \times 10^{-5}$
$D^+ \rightarrow a_1^0 \ell \nu$	$[1.39 \pm 0.18]$	2.37 ± 0.34	3.76 ± 0.52	--	$1.47^{+0.55}_{-0.44}$	$] \times 10^{-5}$
$D^0 \rightarrow b_1^- \ell \nu$	$[0.70 \pm 0.11]$	1.18 ± 0.19	1.88 ± 0.30	--	--	$] \times 10^{-5}$
$D^+ \rightarrow b_1^0 \ell \nu$	$[0.91 \pm 0.15]$	1.56 ± 0.25	2.47 ± 0.40	--	--	$] \times 10^{-5}$
$D^0 \rightarrow K_1^-(1270)\ell\nu$	$[2.22 \pm 0.03]$	4.56 ± 0.09	6.78 ± 0.12	5.34 ± 0.21	--	$] \times 10^{-3}$
$D^+ \rightarrow K_1^0(1270)\ell\nu$	$[6.56 \pm 0.10]$	10.30 ± 0.17	16.86 ± 0.27	14.07 ± 1.22	--	$] \times 10^{-3}$
$D_s^+ \rightarrow K_1^0(1270)\ell\nu$	$[0.66 \pm 0.02]$	1.00 ± 0.03	1.66 ± 0.05	1.25 ± 0.11	--	$] \times 10^{-3}$
$D^0 \rightarrow K_1^-(1400)\ell\nu$	$[0.34 \pm 0.02]$	0.48 ± 0.03	0.82 ± 0.05	0.85 ± 0.02	--	$] \times 10^{-3}$
$D^+ \rightarrow K_1^0(1400)\ell\nu$	$[0.50 \pm 0.04]$	0.78 ± 0.04	1.28 ± 0.08	1.27 ± 0.10	--	$] \times 10^{-3}$
$D_s^+ \rightarrow K_1^0(1400)\ell\nu$	$[0.06 \pm 0.01]$	0.10 ± 0.01	0.16 ± 0.02	0.14 ± 0.01	--	$] \times 10^{-3}$

TABLE X: The same as Table VIII but related to fit function $F^{(3)}$.

Process	Br_T	Br_L	Br_{tot} (This work)	Br_{tot} [26]	Br_{tot} [27]	
$D^0 \rightarrow a_1^- \ell \nu$	$[1.20 \pm 0.16]$	2.38 ± 0.36	3.58 ± 0.52	--	$1.11^{+0.41}_{-0.34}$	$] \times 10^{-5}$
$D^+ \rightarrow a_1^0 \ell \nu$	$[1.57 \pm 0.19]$	3.16 ± 0.44	4.73 ± 0.63	--	$1.47^{+0.55}_{-0.44}$	$] \times 10^{-5}$
$D^0 \rightarrow b_1^- \ell \nu$	$[0.67 \pm 0.10]$	0.80 ± 0.13	1.47 ± 0.32	--	--	$] \times 10^{-5}$
$D^+ \rightarrow b_1^0 \ell \nu$	$[0.87 \pm 0.14]$	1.04 ± 0.16	1.91 ± 0.30	--	--	$] \times 10^{-5}$
$D^0 \rightarrow K_1^-(1270)\ell\nu$	$[3.18 \pm 0.06]$	5.74 ± 0.10	8.92 ± 0.16	5.34 ± 0.21	--	$] \times 10^{-3}$
$D^+ \rightarrow K_1^0(1270)\ell\nu$	$[8.57 \pm 0.13]$	11.16 ± 0.19	19.73 ± 0.32	14.07 ± 1.22	--	$] \times 10^{-3}$
$D_s^+ \rightarrow K_1^0(1270)\ell\nu$	$[0.96 \pm 0.03]$	1.31 ± 0.05	2.27 ± 0.08	1.25 ± 0.11	--	$] \times 10^{-3}$
$D^0 \rightarrow K_1^-(1400)\ell\nu$	$[0.38 \pm 0.02]$	0.55 ± 0.05	0.93 ± 0.07	0.85 ± 0.02	--	$] \times 10^{-3}$
$D^+ \rightarrow K_1^0(1400)\ell\nu$	$[0.56 \pm 0.04]$	0.90 ± 0.06	1.46 ± 0.10	1.46 ± 0.10	--	$] \times 10^{-3}$
$D_s^+ \rightarrow K_1^0(1400)\ell\nu$	$[0.08 \pm 0.01]$	0.11 ± 0.02	0.19 ± 0.03	0.14 ± 0.01	--	$] \times 10^{-3}$

VIII- XI are calculated for $\theta_K = -(34 \pm 13)^\circ$. For a better analysis, the θ_K dependence of the branching ratio values of $D \rightarrow K_1(1270)\ell\nu$ is displaced in Fig. 4.

TABLE XI: The same as Table VIII but related to fit function $F^{(4)}$.

Process	Br_T	Br_L	Br_{tot} (This work)	Br_{tot} [26]	Br_{tot} [27]	
$D^0 \rightarrow a_1^- \ell \nu$	$[1.19 \pm 0.16]$	2.38 ± 0.36	3.57 ± 0.52	--	$1.11^{+0.41}_{-0.34}$	$] \times 10^{-5}$
$D^+ \rightarrow a_1^0 \ell \nu$	$[1.56 \pm 0.19]$	3.14 ± 0.44	4.70 ± 0.63	--	$1.47^{+0.55}_{-0.44}$	$] \times 10^{-5}$
$D^0 \rightarrow b_1^- \ell \nu$	$[0.74 \pm 0.12]$	1.25 ± 0.20	1.99 ± 0.32	--	--	$] \times 10^{-5}$
$D^+ \rightarrow b_1^0 \ell \nu$	$[0.96 \pm 0.16]$	1.63 ± 0.26	2.59 ± 0.42	--	--	$] \times 10^{-5}$
$D^0 \rightarrow K_1^-(1270) \ell \nu$	$[3.32 \pm 0.06]$	5.98 ± 0.11	9.30 ± 0.17	5.34 ± 0.21	--	$] \times 10^{-3}$
$D^+ \rightarrow K_1^0(1270) \ell \nu$	$[8.93 \pm 0.14]$	11.68 ± 0.20	20.61 ± 0.34	14.07 ± 1.22	--	$] \times 10^{-3}$
$D_s^+ \rightarrow K_1^0(1270) \ell \nu$	$[1.01 \pm 0.03]$	1.37 ± 0.06	2.38 ± 0.09	1.25 ± 0.11	--	$] \times 10^{-3}$
$D^0 \rightarrow K_1^-(1400) \ell \nu$	$[0.36 \pm 0.02]$	0.52 ± 0.04	0.88 ± 0.06	0.85 ± 0.02	--	$] \times 10^{-3}$
$D^+ \rightarrow K_1^0(1400) \ell \nu$	$[0.53 \pm 0.03]$	0.85 ± 0.05	1.38 ± 0.08	1.27 ± 0.10	--	$] \times 10^{-3}$
$D_s^+ \rightarrow K_1^0(1400) \ell \nu$	$[0.07 \pm 0.01]$	0.10 ± 0.01	0.17 ± 0.02	0.14 ± 0.01	--	$] \times 10^{-3}$

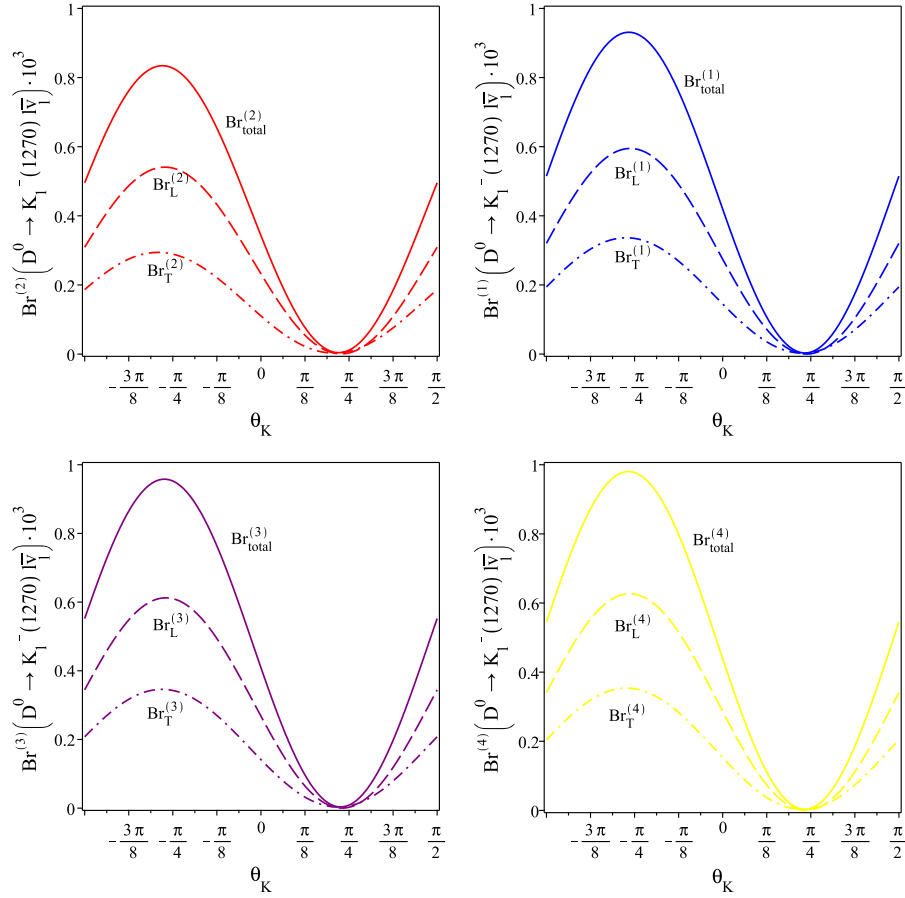


FIG. 4: The θ_K dependence of branching ratio values of $D \rightarrow K_1(1270)\ell\nu$ decay. The solid, dash and dot-dashed lines depict the total, longitudinal and transverse branching ratios, respectively. Blue, red, purple and yellow plots show the results using the form factors fitted to $F^{(i)}$ ($i = 1, \dots, 4$).

B. Analysis of nonleptonic decays

Finally, we want to evaluate the branching ratio values for the nonleptonic $D^0 \rightarrow K_1^-(1270, 1400)\pi^+$ and $D^+ \rightarrow K_1^0(1270, 1400)\pi^+$ decays. The decay width of these nonleptonic processes is given by:

$$\Gamma(D \rightarrow K_1\pi) = \frac{1}{16\pi m_D^3} |\mathcal{M}|^2 \sqrt{\lambda'} \quad (25)$$

where $\lambda' = m_D^4 + m_{K_1}^4 + m_\pi^4 - 2m_{K_1}^2 m_D^2 - 2m_\pi^2 m_D^2 - 2m_\pi^2 m_{K_1}^2$. For these decay, the effective Hamiltonian is given as

$$H_{eff} = \frac{G_F}{\sqrt{2}} V_{cs}^* V_{ud} \left(C_1 + \frac{C_2}{N_c} \right) (\bar{s}c)_{V-A} (\bar{u}d)_{V-A} + h.c.. \quad (26)$$

In this Hamiltonian, $(\bar{s}c)_{V-A} (\bar{u}d)_{V-A} = [\bar{s} \gamma^\mu (1 - \gamma_5) c][\bar{u} \gamma^\mu (1 - \gamma_5) d]$, and C_1 and C_2 are Wilson coefficients. $N_c = 3$ is the number of colors in QCD. Using the factorization method, we obtain the amplitude \mathcal{M} as follows:

$$\mathcal{M} = \sqrt{2} G_F V_{cs}^* V_{ud} [e_1 f_\pi m_{K_1} (\varepsilon^* \cdot p_\pi) V_0(m_\pi^2)], \quad (27)$$

where f_π is the pion decay constant, and $e_1 = C_1 + \frac{1}{N_c} C_2$. The decay width for $D \rightarrow K_1 \pi$ can be written as [26]:

$$\Gamma(D \rightarrow K_1 \pi) = \frac{G_F^2}{32 \pi m_D^3} |V_{cs}|^2 |V_{ud}|^2 e_1^2 f_\pi^2 \lambda^{\frac{3}{2}} |V_0(m_\pi^2)|^2. \quad (28)$$

To estimate $\Gamma(D \rightarrow K_1 \pi)$, we use $f_\pi = 0.13$ GeV, $m_\pi = 0.14$ GeV, $V_{ud} = 0.97$, and $V_{cs} = 0.99$ [40]. For obtaining e_1 , the values $C_1(m_c) = 1.26$ and $C_2(m_c) = -0.51$ are chosen, corresponding to the results for the Wilson coefficients obtained at the leading order in renormalization group improved perturbation theory at $\mu = m_c \simeq 1.4$ GeV, in correspondence to $\alpha_s(M_Z) = 0.118$ [44]. Using four fit functions $F^{(i)} (i = 1, \dots, 4)$, the values for the branching ratios of the nonleptonic decays $D^0 \rightarrow K_1^-(1270)\pi^+$, $D^0 \rightarrow K_1^-(1400)\pi^+$, $D^+ \rightarrow K_1^0(1270)\pi^+$ and $D^+ \rightarrow K_1^0(1400)\pi^+$ are obtained and presented in Tables XIII. This table also contains the results estimated by the 3PSR method and experiment. As can be seen in Table XII, our results for three fit functions are close to each other.

TABLE XII: The branching ratio values of the nonleptonic $D^0 \rightarrow K_1^-(1270)\pi^+$, $D^0 \rightarrow K_1^-(1400)\pi^+$, $D^+ \rightarrow K_1^0(1270)\pi^+$ and $D^+ \rightarrow K_1^0(1400)\pi^+$ decays via the different methods and experiment. Our results are related to four fit functions.

Process	This work ($F^{(1)}$)	This work ($F^{(2)}$)	This work ($F^{(3)}$)	This work ($F^{(4)}$)	3PSR [26]	Exp [40, 45]
$Br(D^0 \rightarrow K_1^-(1270)\pi^+) \times 10^{-2}$	2.55 ± 0.15	2.57 ± 0.16	2.54 ± 0.15	2.65 ± 0.16	2.26 ± 0.18	1.6 ± 0.8
$Br(D^0 \rightarrow K_1^-(1400)\pi^+) \times 10^{-2}$	0.18 ± 0.03	0.16 ± 0.03	0.15 ± 0.02	0.17 ± 0.03	0.26 ± 0.02	< 1.2
$Br(D^+ \rightarrow K_1^0(1270)\pi^+) \times 10^{-2}$	6.19 ± 0.18	6.42 ± 0.20	6.17 ± 0.20	6.44 ± 0.21	5.85 ± 0.37	< 0.7
$Br(D^+ \rightarrow K_1^0(1400)\pi^+) \times 10^{-2}$	1.49 ± 0.10	1.33 ± 0.04	1.30 ± 0.03	1.40 ± 0.08	1.71 ± 0.13	3.8 ± 1.3

In summary, we investigated the form factors of the semileptonic $D_{(s)}$ decay into the $a_1, b_1, K_1(1270), K_1(1400)$ axial vector mesons in the LCSR approach up to the twist-3 LCDAs. In order to extend our results to the full physical region, we used four fit functions for parametrization of the form factors. There was not any significant change in our results using four fit functions. The branching ratio values of the semileptonic $D^0 \rightarrow a_1^-(b_1^-)\ell^+\nu$, $D^+ \rightarrow a_1^0(b_1^0)\ell^+\nu$, $D_s^+ \rightarrow K_1^0\ell^+\nu$ as well as $D^+ \rightarrow K_1^0\ell^+\nu$ decays were evaluated. Using the QCD factorization method, the nonleptonic decays $D \rightarrow K_1(1270, 1400)\pi$ were considered and their branching ratio values were predicted. A comparison was made between our results and other method predictions and also the experimental values.

Appendix A: Twist Function Definitions

In this appendix, we present the definitions for the two- and three-parton LCDAs as well as the twist functions. Two-particle chiral-even distribution amplitudes are given by [39]:

$$\begin{aligned}\langle a_1^-(p', \varepsilon) | \bar{d}(x) \gamma_\mu \gamma_5 u(0) | 0 \rangle &= i f_{a_1^-} m_{a_1^-} \int_0^1 du e^{iup' \cdot x} \left\{ p'_\mu \frac{\varepsilon^* \cdot x}{p' \cdot x} \Phi_{\parallel}(u) + \left(\varepsilon_\mu^* - p'_\mu \frac{\varepsilon^* \cdot x}{p' \cdot x} \right) g_{\perp}^{(a)}(u) + \mathcal{O}(x^2) \right\}, \\ \langle a_1^-(p', \varepsilon) | \bar{d}(x) \gamma_\mu u(0) | 0 \rangle &= -i f_{a_1^-} m_{a_1^-} \times \epsilon_{\mu\nu\rho\sigma} \varepsilon^{*\nu} p'^\rho x^\sigma \int_0^1 du e^{iup' \cdot x} \left\{ \frac{g_{\perp}^{(v)}(u)}{4} + \mathcal{O}(x^2) \right\},\end{aligned}\quad (A1)$$

also, two-particle chiral-odd distribution amplitudes are defined by:

$$\begin{aligned}\langle a_1^-(p', \varepsilon) | \bar{d}(x) \sigma_{\mu\nu} \gamma_5 u(0) | 0 \rangle &= f_{a_1^-}^\perp \int_0^1 du e^{iup' \cdot x} \left\{ (\varepsilon_\mu^* p'_\nu - \varepsilon_\nu^* p'_\mu) \Phi_{\perp}(u) + \frac{m_{a_1^-}^2 \varepsilon^* \cdot x}{(p' \cdot x)^2} (p'_\mu x_\nu - p'_\nu x_\mu) \bar{h}_{\parallel}^{(t)} + \mathcal{O}(x^2) \right\}, \\ \langle a_1^-(p', \varepsilon) | \bar{d}(x) \gamma_5 u(0) | 0 \rangle &= f_{a_1^-}^\perp m_{a_1^-}^2 (\varepsilon^* \cdot x) \int_0^1 du e^{iup' \cdot x} \left\{ \frac{h_{\parallel}^{(p)}(u)}{2} + \mathcal{O}(x^2) \right\}.\end{aligned}\quad (A2)$$

In these expressions, $f_{a_1^-}$ and $f_{a_1^-}^\perp$ are decay constants of the axial vector meson a_1^- . We set $f_{a_1^-}^\perp = f_{a_1^-}$ in $\mu = 1$ GeV, such that we have

$$\langle a_1^-(p', \varepsilon) | \bar{d}(0) \sigma_{\mu\nu} \gamma_5 u(0) | 0 \rangle = a_0^{\perp, a_1^-} f_{a_1^-} (\varepsilon_\mu^* p'_\nu - \varepsilon_\nu^* p'_\mu), \quad (A3)$$

where a_0^\perp refers to the zeroth Gegenbauer moments of Φ_{\perp} . It should be noted that $f_{a_1^-}$ is scale-independent and conserves G -parity, but $f_{a_1^-}^\perp$ is scale-dependent and violates G -parity.

We take into account the approximate forms of twist-2 distributions for the a_1^- meson to be [28]

$$\Phi_{\parallel}(u) = 6u\bar{u} \left[1 + 3a_1^{\parallel} \xi + a_2^{\parallel} \frac{3}{2} (5\xi^2 - 1) \right], \quad (A4)$$

$$\Phi_{\perp}(u) = 6u\bar{u} \left[a_0^{\perp} + 3a_1^{\perp} \xi + a_2^{\perp} \frac{3}{2} (5\xi^2 - 1) \right], \quad (A5)$$

where $\xi = 2u - 1$.

For the relevant two-parton twist-3 chiral-even LCDAs, we take the approximate expressions up to conformal spin 9/2 [28]:

$$\begin{aligned}g_{\perp}^{(a)}(u) &= \frac{3}{4} (1 + \xi^2) + \frac{3}{2} a_1^{\parallel} \xi^3 + \left(\frac{3}{7} a_2^{\parallel} + 5\zeta_{3, a_1^-}^V \right) (3\xi^2 - 1) \\ &+ \left(\frac{9}{112} a_2^{\parallel} + \frac{105}{16} \zeta_{3, a_1^-}^A - \frac{15}{64} \zeta_{3, a_1^-}^V \omega_{a_1^-}^V \right) (35\xi^4 - 30\xi^2 + 3) \\ &+ 5 \left[\frac{21}{4} \zeta_{3, a_1^-}^V \sigma_{a_1^-}^V + \zeta_{3, a_1^-}^A \left(\lambda_{a_1^-}^A - \frac{3}{16} \sigma_{a_1^-}^A \right) \right] \xi (5\xi^2 - 3) \\ &- \frac{9}{2} a_1^{\perp} \tilde{\delta}_+ \left(\frac{3}{2} + \frac{3}{2} \xi^2 + \ln u + \ln \bar{u} \right) - \frac{9}{2} a_1^{\perp} \tilde{\delta}_- (3\xi + \ln \bar{u} - \ln u),\end{aligned}\quad (A6)$$

$$\begin{aligned}g_{\perp}^{(v)}(u) &= 6u\bar{u} \left\{ 1 + \left(a_1^{\parallel} + \frac{20}{3} \zeta_{3, a_1^-}^A \lambda_{a_1^-}^A \right) \xi \right. \\ &+ \left[\frac{1}{4} a_2^{\parallel} + \frac{5}{3} \zeta_{3, a_1^-}^V \left(1 - \frac{3}{16} \omega_{a_1^-}^V \right) + \frac{35}{4} \zeta_{3, a_1^-}^A \right] (5\xi^2 - 1) \\ &+ \frac{35}{4} \left(\zeta_{3, a_1^-}^V \sigma_{a_1^-}^V - \frac{1}{28} \zeta_{3, a_1^-}^A \sigma_{a_1^-}^A \right) \xi (7\xi^2 - 3) \Big\} \\ &- 18 a_1^{\perp} \tilde{\delta}_+ (3u\bar{u} + \bar{u} \ln \bar{u} + u \ln u) - 18 a_1^{\perp} \tilde{\delta}_- (u\bar{u} \xi + \bar{u} \ln \bar{u} - u \ln u),\end{aligned}\quad (A7)$$

where

$$\tilde{\delta}_{\pm} = \frac{f_{a_1^-}^{\perp}}{f_{a_1^-}} \frac{m_u \pm m_d}{m_{a_1^-}}, \quad \zeta_{3,a_1^-}^{V(A)} = \frac{f_{3a_1^-}^{V(A)}}{f_{a_1^-} m_{a_1^-}}. \quad (\text{A8})$$

Three-particle distribution amplitudes are defined as:

$$\begin{aligned} \langle a_1^-(p', \varepsilon) | \bar{d}(x) \gamma_{\alpha} \gamma_5 g_s G_{\mu\nu}(ux) u(0) | 0 \rangle &= p'_{\alpha} (p'_{\nu} \varepsilon_{\mu}^* - p'_{\mu} \varepsilon_{\nu}^*) f_{3a_1^-}^A \mathcal{A} + \dots, \\ \langle a_1^-(p', \varepsilon) | \bar{d}(x) \gamma_{\alpha} g_s \tilde{G}_{\mu\nu}(ux) u(0) | 0 \rangle &= i p'_{\alpha} (p'_{\mu} \varepsilon_{\nu}^* - p'_{\nu} \varepsilon_{\mu}^*) f_{3a_1^-}^V \mathcal{V} + \dots, \end{aligned} \quad (\text{A9})$$

where $\tilde{G}_{\mu\nu} = \frac{1}{2} \epsilon_{\mu\nu\rho\lambda} G^{\rho\lambda}$.

The three-parton chiral-even distribution amplitudes \mathcal{A} and \mathcal{V} in Eq. (A9) are defined as:

$$\begin{aligned} \mathcal{A} &= \int \mathcal{D}\underline{\alpha} e^{ip' \cdot x(\alpha_1 + u\alpha_3)} \mathcal{A}(\alpha_i), \\ \mathcal{V} &= \int \mathcal{D}\underline{\alpha} e^{ip' \cdot x(\alpha_1 + u\alpha_3)} \mathcal{V}(\alpha_i), \end{aligned} \quad (\text{A10})$$

where $\mathcal{A}(\alpha_i)$ and $\mathcal{V}(\alpha_i)$ can be approximately written as [28]:

$$\begin{aligned} \mathcal{A}(\alpha_i) &= 5040(\alpha_1 - \alpha_2)\alpha_1\alpha_2\alpha_3^2 + 360\alpha_1\alpha_2\alpha_3^2 \left[\lambda_{a_1^-}^A + \frac{\sigma_{a_1^-}^A}{2}(7\alpha_3 - 3) \right], \\ \mathcal{V}(\alpha_i) &= 360\alpha_1\alpha_2\alpha_3^2 \left[1 + \frac{\omega_{a_1^-}^V}{2}(7\alpha_3 - 3) \right] + 5040(\alpha_1 - \alpha_2)\alpha_1\alpha_2\alpha_3^2 \sigma_{a_1^-}^V, \end{aligned} \quad (\text{A11})$$

In these expressions α_1 , α_2 , and α_3 are the momentum fractions carried by d , \bar{u} quarks and gluon, respectively, in the axial vector meson a_1^- . The integration measure is defined as:

$$\int \mathcal{D}\underline{\alpha} \equiv \int_0^1 d\alpha_1 \int_0^1 d\alpha_2 \int_0^1 d\alpha_3 \delta(1 - \sum \alpha_i). \quad (\text{A12})$$

Appendix B: Form Factor Expressions

In this appendix, the explicit expressions for the form factors of the semileptonic $D^0 \rightarrow a_1^- \ell^+ \nu$ decay are presented.

$$\begin{aligned}
V_1(q^2) &= -\frac{m_c f_{a_1^-}^\perp}{8m_{D^0}^2(m_{D^0} - m_{a_1^-})f_{D^0}} e^{\frac{m_{D^0}^2}{M^2}} \left\{ \hat{\mathcal{L}} \left[7 \frac{\Phi_\perp(u) \delta_1(u)}{2u} + 2m_{a_1^-}^2 \frac{h_\parallel^{(p)}(u)}{u} - 3 \frac{m_c m_{a_1^-} f_{a_1^-}}{f_{a_1^-}^\perp} \frac{g_\perp^{(a)}(u)}{u} \right. \right. \\
&\quad \left. \left. - m_{a_1^-}^2 \frac{\bar{h}_\parallel^{(t)(ii)}(u)}{u^2} (7 + \frac{\delta_2(u)}{M^2}) - 4 \frac{m_c m_{a_1^-}^3 \phi_b^{ii}(u)}{M^2 u^2} \right] e^{s(u)} + 4 \frac{m_c m_{a_1^-}^2}{M^2 f_{a_1^-}^\perp} \hat{\mathcal{L}} \left[\int \mathcal{D}\alpha \left(\frac{\delta_3(\alpha_i)}{\kappa^2} \right) e^{s(\kappa)} \right] \right\}, \\
V_2(q^2) &= \frac{2m_c(m_{D^0} - m_{a_1^-})f_{a_1^-}^\perp}{m_{D^0}^2 f_{D^0}} e^{\frac{m_{D^0}^2}{M^2}} \left\{ \hat{\mathcal{L}} \left[8 \frac{\Phi_\perp(u)}{u} + 2 \frac{m_c m_{a_1^-} f_{a_1^-}}{M^2 f_{a_1^-}^\perp} \frac{\phi_a(u)}{u^2} + 2m_{a_1^-}^2 (1 + 2u) \frac{h_\parallel^{(p)}(u)}{u} \right. \right. \\
&\quad \left. \left. + 8 \frac{m_c m_{a_1^-} f_{a_1^-}}{M^2 f_{a_1^-}^\perp} \frac{\Phi_\parallel^{(i)}(u)}{u^2} - 2 \frac{m_{a_1^-}^2}{M^2} \frac{\bar{h}_\parallel^{(t)(ii)}(u)}{u^3} \left(\frac{\delta_4(u)}{M^2} - 7u - 2 \right) - 8 \frac{m_c m_{a_1^-}^3 \phi_b^{ii}(u)}{M^4 u^3} \right] e^{s(u)} \right\} \\
V_0(q^2) - V_3(q^2) &= q^2 \frac{m_c f_{a_1^-}^\perp}{8m_D^2 m_{a_1^-} f_D} e^{\frac{m_D^2}{M^2}} \left\{ \hat{\mathcal{L}} \left[8 \frac{\Phi_\perp(u)}{u} + 2 \frac{m_c m_{a_1^-} f_{a_1^-}}{M^2 f_{a_1^-}^\perp} \frac{\phi_a(u)}{u^2} - 4m_{a_1^-}^2 \frac{h_\parallel^{(p)}(u)}{u} (1 - u) \right. \right. \\
&\quad \left. \left. + 16 \frac{m_c m_{a_1^-} f_{a_1^-}}{M^2 f_{a_1^-}^\perp} \frac{\Phi_\parallel^{(i)}(u)}{u^2} + 2m_{a_1^-}^2 \frac{\bar{h}_\parallel^{(t)(ii)}(u)}{u^3} \left(\frac{\delta_4(u) - M^2(7u + 2)}{M^4} \right) - 4 \frac{m_c m_{a_1^-}^3 f_{a_1^-}}{M^4 f_{a_1^-}^\perp} \right. \right. \\
&\quad \left. \left. \times \frac{\phi_b^{ii}(u)(1 - u)}{u^4} \right] e^{s(u)} \right\},
\end{aligned}$$

where

$$\begin{aligned}
\hat{\mathcal{L}} &= \int_{u_0}^1 du, \\
u_0 &= \frac{1}{2m_{a_1^-}^2} \left[\sqrt{(s_0 - m_{a_1^-}^2 - q^2)^2 + 4m_{a_1^-}^2(m_c^2 - q^2)} - (s_0 - m_{a_1^-}^2 - q^2) \right], \\
s(u) &= -\frac{1}{M^2 u} \left[m_c^2 + u \bar{u} m_{a_1^-}^2 - \bar{u} q^2 \right], \\
\delta_1(u) &= m_{a_1^-}^2 (u + 2) + \frac{m_c^2}{u} + \frac{q^2}{u}, \\
\delta_2(u) &= m_{a_1^-}^2 u + \frac{m_c^2}{u} - \frac{q^2}{u}, \\
\delta_3(\alpha_i) &= f_{3a_1^-}^A \mathcal{A}(\alpha_i) - f_{3a_1^-}^V \mathcal{V}(\alpha_i), \\
\delta_4(u) &= \frac{m_c^2}{u} (2 - 16u) + 2m_{a_1^-}^2 (2 + u(1 - u)) - \frac{q^2}{u} (15 + 12u), \\
h^{(i)}(u) &\equiv \int_0^u h(v) dv, \\
h^{(ii)}(u) &\equiv \int_0^u dv \int_0^v d\omega h(\omega), \\
\phi_a &= \int_0^u \left[\Phi_\parallel - g_\perp^{(a)}(v) \right] dv, \\
\kappa &= \alpha_1 + u\alpha_3.
\end{aligned}$$

-
- [1] M. Artuso, B. Meadows and A. A. Petrov, *Ann. Rev. Nucl. Part. Sci* **58**, 249 (2008).
 - [2] T. Feldmann, B. Mueller and D. Seidel, *JHEP* **1708**, 105 (2017).
 - [3] T. Palmer and J. O. Eeg, *Phys. Rev. D* **89**, 034013 (2014).
 - [4] V. L. Chernyak and A. R. Zhitnitsky, *Phys. Rep.* **112**, 173 (1984).
 - [5] I. I. Balitsky, V. M. Braun and A. V. Kolesnichenko, *Nucl. Phys. B* **312**, 509 (1989).
 - [6] V. M. Braun and I. E. Filyanov, *Z. Phys. C* **44**, 157 (1989).
 - [7] V. L. Chernyak and I. R. Zhitnitsky, *Nucl. Phys. B* **345**, 137 (1990).
 - [8] V. M. Braun and I. E. Filyanov, *Z. Phys. C* **48**, 239 (1990).
 - [9] N. R. Soni and J. N. Pandya, *Phys. Rev. D* **96**, 016017 (2017).
 - [10] N. R. Soni, M. A. Ivanov, J. G. Korner, J. N. Pandya, P. Santorelli and C. T. Tran, arXiv:1810.11907 [hep-ph].
 - [11] J. Zhang, C. X. Yue, C. H. Li, *Eur. Phys. J. C* **78**, 695 (2018).
 - [12] A. Khodjamirian, R. Ruckl, S. Weinzierl, C. Winhart, and O. I. Yakovlev, *Phys. Rev. D* **62**, 114002 (2000).
 - [13] P. Ball, *Phys. Lett. B* **641**, 50 (2006).
 - [14] H. B. Fu, X. Yang, R. Lu, L. Zeng, W. Cheng and X. G. Wu, arXiv:1808.06412 [hep-ph].
 - [15] W. Y. Wang, Y. L. Wu, and M. Zhong, *Phys. Rev. D* **67**, 014024 (2003).
 - [16] A. Abada et al. (SPQcdR collaboration), *Nucl. Phys. Proc. Suppl.* **119**, 625 (2003).
 - [17] C. Aubin et al. (Fermilab Lattice), *Phys. Rev. Lett.* **94**, 011601 (2005).
 - [18] C. Bernard et al., *Phys. Rev. D* **80**, 034026 (2009).
 - [19] I. Bediaga and M. Nielsen, *Phys. Rev. D* **68**, 036001 (2003).
 - [20] T. M. Aliev, V. L. Eletsky, and Ya. I. Kogan, *Sov. J. Nucl. Phys.* **40**, 527 (1984).
 - [21] P. Ball, V. M. Braun, and H. G. Dosch, *Phys. Rev. D* **44**, 3567 (1991).
 - [22] P. Ball, *Phys. Rev. D* **48**, 3190 (1993).
 - [23] A. A. Ovchinnikov and V. A. Slobodenyuk, *Z. Phys. C* **44**, 433 (1989); V. N. Baier and A. Grozin, *Z. Phys. C* **47**, 669 (1990).
 - [24] D. S. Du, J. W. Li, and M. Z. Yang, *Eur. Phys. J. C* **37**, 137 (2004).
 - [25] M. Z. Yang, *Phys. Rev. D* **73**, 034027 (2006); **73**, 079901(E) (2006).
 - [26] R. Khosravi, K. Azizi and N. Ghahramany, *Phys. Rev. D* **79**, 036004 (2009).
 - [27] Y. Zuo et al, *Int. J. Mod. Phys. A* **31**, 1650116 (2016).
 - [28] K. Yang, *Nucl. Phys. B* **776**, 187 (2007).
 - [29] L. Burakovsky and T. Goldman, *Phys. Rev. D* **57**, 2879 (1998).
 - [30] M. Suzuki, *Phys. Rev. D* **47**, 1252 (1993).
 - [31] H. Y. Cheng, *Phys. Rev. D* **67**, 094007 (2003).
 - [32] H. Hatanaka, K. C. Yang, *Phys. Rev. D* **77**, 094023 (2008).
 - [33] H. Dag, A. Ozpineci and M. T. Zeyrek, *J. Phys. G* **38**, 015002 (2011).
 - [34] M. Bayar and K. Azizi, *Eur. Phys. J. C* **61**, 401 (2009).
 - [35] K. C. Yang, *Phys. Rev. D* **78**, 034018 (2008).
 - [36] V. Bashiry and K. Azizi, *JHEP* **1001**, 033 (2010).
 - [37] F. Falahati and A. Zahedidareshouri, *Phys. Rev. D* **90**, 075002 (2014).
 - [38] H. Hatanaka and K. C. Yang, *Phys. Rev. D* **78**, 074007 (2008).
 - [39] K. Yang, *Phys. Rev. D* **78**, 034018 (2008).
 - [40] C. Patrignani et al. (Particle Data Group), *Chin. Phys. C* **40**, 100001 (2016).
 - [41] H. Mutuk, arXiv: 1807.08511 [hep-ph].
 - [42] C. Bourrely, I. Caprini, and L. Lellouch, *Phys. Rev. D* **79**, 013008 (2009).
 - [43] H.Y. Cheng, C.K. Chua, C.W. Hwang, *Phys. Rev. D* **69**, 074025 (2004).
 - [44] G. Buchalla, A.J. Buras, M.E. Lautenbacher, *Rev. Mod. Phys.* **68**, 1125 (1996).
 - [45] C. Amsler et al. (Particle Data Group), *Phys. Lett. B* **667**, 1 (2008).